Carnegie Observatories Astrophysics Series, Vol. 3:
Clusters of Galaxies: Probes of Cosmological Structure and Galaxy Evolution, 2004
ed. J. S. Mulchaey, A. Dressler, and A. Oemler (Cambridge: Cambridge Univ. Press)

The Stellar Content of Galaxy Clusters

ROGER L. DAVIES
Astrophysics, University of Oxford

Abstract

Clusters of galaxies are well-defined laboratories in which to study the evolution of the stellar content of galaxies. Direct detections of individual stars in intracluster space, as well as measurements of the diffuse light between galaxies, indicate that the gravitational interactions experienced by galaxies in clusters, with each other and with the cluster potential, result in 10%–20% of the stars being expelled into the intracluster space. I consider the properties of cluster galaxies as a function of position and local density within clusters and as a function of redshift: the color-magnitude relation, star formation rate, fundamental plane, age, and metalicity. These data strongly suggest that the population of luminous, high-velocity dispersion galaxies in rich clusters are old and form a metalicity sequence. Furthermore the increasing enhancement of magnesium abundance in high-dispersion galaxies implies a short star formation time scale. These observations suggest that massive, early-type galaxies in clusters formed at high redshift by monolithic collapse and appear counter to the expectations of hierarchical models of galaxy assembly. In lower luminosity ($\sigma < 150$ km s^{-1}) cluster galaxies, galaxies on the periphery of clusters, and galaxies in lower density regions, secondary star formation played an important role in galaxy evolution, consistent with hierarchical assembly. I illustrate how we can attempt to order the events in galaxy assembly using data from the `SAURON` integral-field spectrograph.

1.1 Introduction

Galaxy clusters have been used for decades in studies of the evolution of galaxies and their stellar populations because they contain large numbers of galaxies at a common distance that inhabit a common environment. Exploring the variation in the systematic properties of galaxies as a function of cluster type, radius within the cluster, and cluster redshift has proved to be a fruitful avenue of research (Schneider, Gunn, & Hoessel 1983; Dressler, Gunn, & Schneider 1985; Binggeli, Tammann, & Sandage 1987). Here I will confine my remarks to galaxies that are luminous (in the brightest two decades of the luminosity function) and that are of early morphological type. The morphology-density relation (Dressler 1980) ensures that this includes the vast majority of luminous galaxies in clusters of appreciable richness. I will not consider the population of dwarf galaxies, although there have been new results in this area recently (e.g., Conselice, Gallagher, & Wyse 2003). I will also not consider the globular cluster populations of cluster galaxies; recent work on the Coma system is reported in Harris et al. (2000).

The current state of knowledge of the stellar content of galaxies leads us to pose the following questions. How and when did cluster galaxies assemble? What physical mechanisms give rise to the global scaling relations found among cluster galaxies? What mechanisms are responsible for the variation in galaxy properties with environment? Can we develop a consistent view of galaxy evolution in clusters from $z = 0.5$ to the present day? In § 1.2 I will describe recent advances in the study of intracluster stars. I will discuss the integrated properties of cluster galaxies and their scaling relations, most of which have been established in clusters, in § 1.3. These relationships span structural properties such as luminosity, radius, and surface brightness, dynamical properties such as velocity dispersion and rotation and stellar population diagnostics such as colors, absorption- and emission-line strengths. Much of our knowledge of cluster galaxies arises from comparisons of these relationships within and among clusters, both locally and at high redshifts. I cannot consider all of these relationships but start by reviewing the trends in the color-magnitude relation (CMR) and star formation rate of galaxies as a function of cluster radius and as a function of redshift. I follow that with a summary of the results on the "fundamental plane," connecting size, dispersion, and surface brightness. Section 1.3 concludes with a discussion of the controversial topic of estimating the age and metalicity of the integrated stellar populations of galaxies using line indices. I will review these, illustrating the discussion with respect to the Fornax cluster and by considering the relative abundances of iron and magnesium. Before summarizing, I illustrate in § 1.4 how integral-field spectroscopy can give us a much clearer picture of the evolution of individual galaxies.

1.2 The Stars between Galaxies

Models of gravitational interactions of cluster galaxies with each other and with the potential of the cluster lead us to expect that stars will be ejected from galaxies into the intracluster space (e.g., Moore et al. 1996). Individual stars have now been detected. Diffuse emission in clusters, with a morphology indicative of tidal interactions between galaxies, has also been detected.

1.2.1 Planetary Nebulae

Using narrow-band imaging centered on the [O III] emission line, Theuns & Warren (1997) identified 10 candidate intergalactic planetary nebulae in the Fornax cluster in three fields chosen well away from any galaxy. Much of the follow-up work has been carried out by groups measuring the distance to clusters using the planetary nebula luminosity function. For example, in the Virgo cluster the current state-of-the-art has been reported by Arnaboldi et al. (2003). They identified intracluster planetary nebulae by imaging with the Subaru Suprime-Cam through two narrow-band filters centered at the redshifted wavelengths of [O III] and Hα. Spectroscopic observations confirmed their success in identifying true planetary nebulae. Based on their identification of 36 intracluster planetary nebulae, of which 25% were assumed to be contaminating background objects, they derived a lower limit of 10% and an upper limit of 40% for the fraction of the *B*-band Virgo cluster light contributed by intracluster stars.

1.2.2 Red Giant Branch Stars

In 1998, Ferguson, Tanvir, & von Hippel used deep imaging on the *Hubble Space Telescope (HST)* to discover red giant branch (RGB) stars in a blank field in the Virgo cluster.

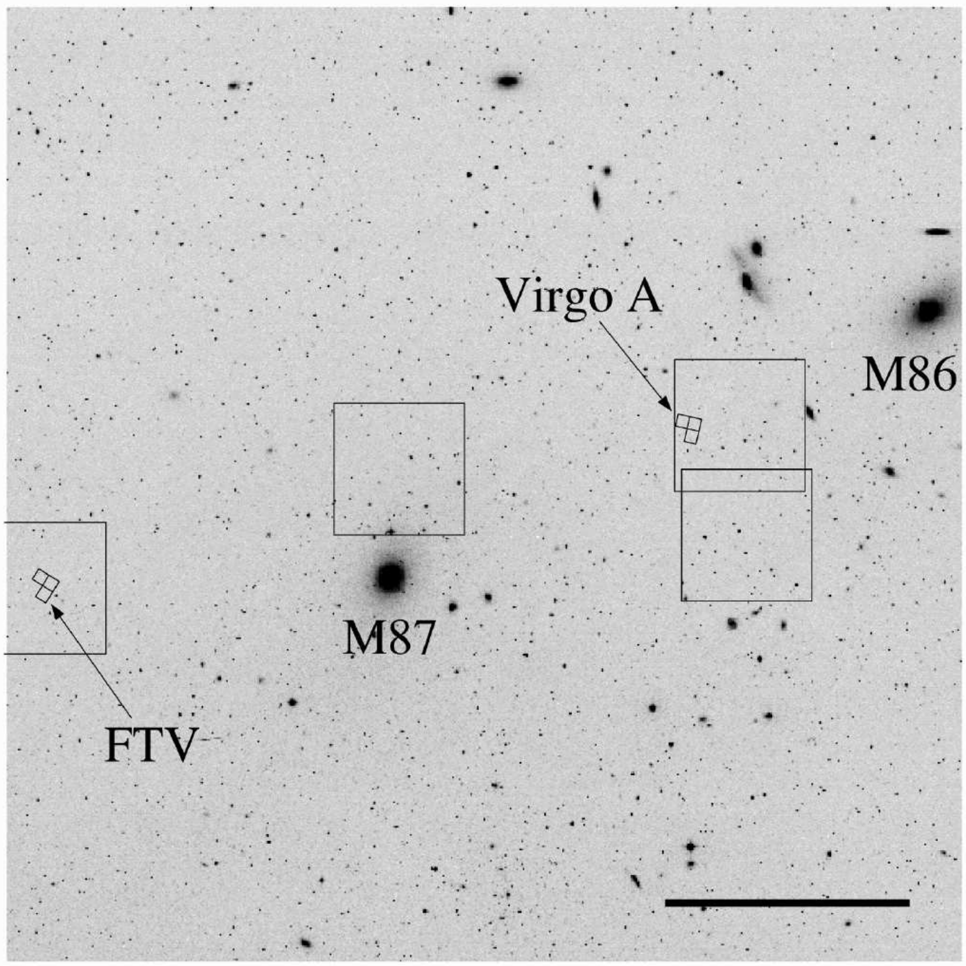

Fig. 1.1. Digitized Sky Survey image of the central region of the Virgo cluster, labeled with the location of the *HST* WFPC2 field used by Durrell et al. (2002) to search for RGB stars (labeled "Virgo A") and that used by Ferguson, Tanvir, & von Hippel (1998). The image is 2° on a side, with North at the top and East to the left. Also shown are the four fields used by Feldmeier et al. (2002) to search for intracluster planetary nebulae. (From Durrell et al. 2002.)

They suggested that the intracluster stars account for roughly one-tenth of the total stellar mass of the cluster. More recent studies (e.g., Durrell et al. 2002) have used deep F814W images to estimate the number of RGB stars in two fields in Virgo using the two Hubble Deep Fields as a control. At magnitudes fainter than $I = 27$ they found an excess of point sources in the Virgo fields. Modeling the luminosity function, they concluded that the tip of the RGB in the intracluster stars is at $I = 27.3$ mag and that the metalicity of the stars spans $-0.8 <$ [Fe/H] < -0.2, consistent with them originating in luminous galaxies. An analysis of the surface density of RGB stars led them to estimate that the intracluster population accounts for 10%–20% of the I-band luminosity of the Virgo cluster. In Figure 1.1, reproduced from Durrell et al. (2002), the fields in which Virgo cluster planetary nebulae and RGB stars have been found are shown on a Digitized Sky Survey image.

These two methods of detecting resolved stars in the Virgo cluster are converging on an estimate of 10%–20% of the stellar mass of the cluster being ejected from galaxies into a diffuse component.

1.2.3 Diffuse Intracluster Light

Attempts to measure a diffuse component of intracluster light have a long history entangled with studies of galaxy clustering and low-surface brightness galaxies. Shectman (1973, 1974) predicted, and attempted to measure, the scale of the fluctuations in the background light from photographic plates scanned with a microdensitometer. In 1991 Uson, Boughn, & Kuhn reported the first measurements of the intergalactic background light in clusters using CCDs, which enabled them to measure down to 2×10^{-4} of the sky background in the R band. Their investigation of Abell 2029 concluded that, between cluster radii of 125–425 kpc, 5%–10% of the cluster light is in a diffuse component. With the advent of large CCDs this method has been used to identify specific components of tidal debris in clusters. For example, V-band imaging to $\mu_V = 26.5$ mag arcsec^{-2} by Feldmeier et al. (2002) revealed an extended plume of material in MKW7 but found no extended tidal arcs (Feldmeier et al. 2004). It seems likely that with the advent of large CCDs this work will expand and confront the varying predictions of the scale and distribution expected for tidal debris in clusters.

1.3 Stars in Galaxies

1.3.1 The Color-Magnitude Relation in Local Clusters

We have known for decades that early-type galaxies in clusters get slighter redder as they become more luminous (Sandage 1972). This is a small effect, seen most clearly in colors that include an ultraviolet band. For example, Visvanathan & Sandage (1977) determined that galaxies in nine groups and clusters obey the same relationship, namely that the $u-V$ color reddens by 0.1 magnitude for each V magnitude increase in brightness. Furthermore, they established that the relationship has a scatter of 0.1 magnitude in color and is common to elliptical and lenticular galaxies alike.

Bower, Lucey, & Ellis (1992) measured U, V, J, and K magnitudes for 94 early-type galaxies in Coma and Virgo. The rms scatter in the measurements was between 1.5%–3.0%. They found no difference between the intrinsic colors of galaxies in the two clusters to a precision of a few percent, checking their result using the distance-independent color-velocity dispersion relation. By carefully estimating the observational error they concluded that the *intrinsic* scatter in colors of galaxies was 3%–4%. This remarkable uniformity of galaxy properties between and within the two clusters, when analyzed using stellar population models (Bruzual 1983), led Bower et al. to conclude that the spheroidal components of early-type galaxies in clusters are unlikely to have formed below a redshift of 2.

The Bower et al. (1992) data extended to no fainter than $B = 16$ mag and therefore included only the first decade of the galaxy luminosity function in the Coma cluster. The fainter Virgo galaxies showed some signs of increased scatter in the CMR but the sample is not numerous enough to draw a definitive conclusion. Terlevich et al. (1999) extended

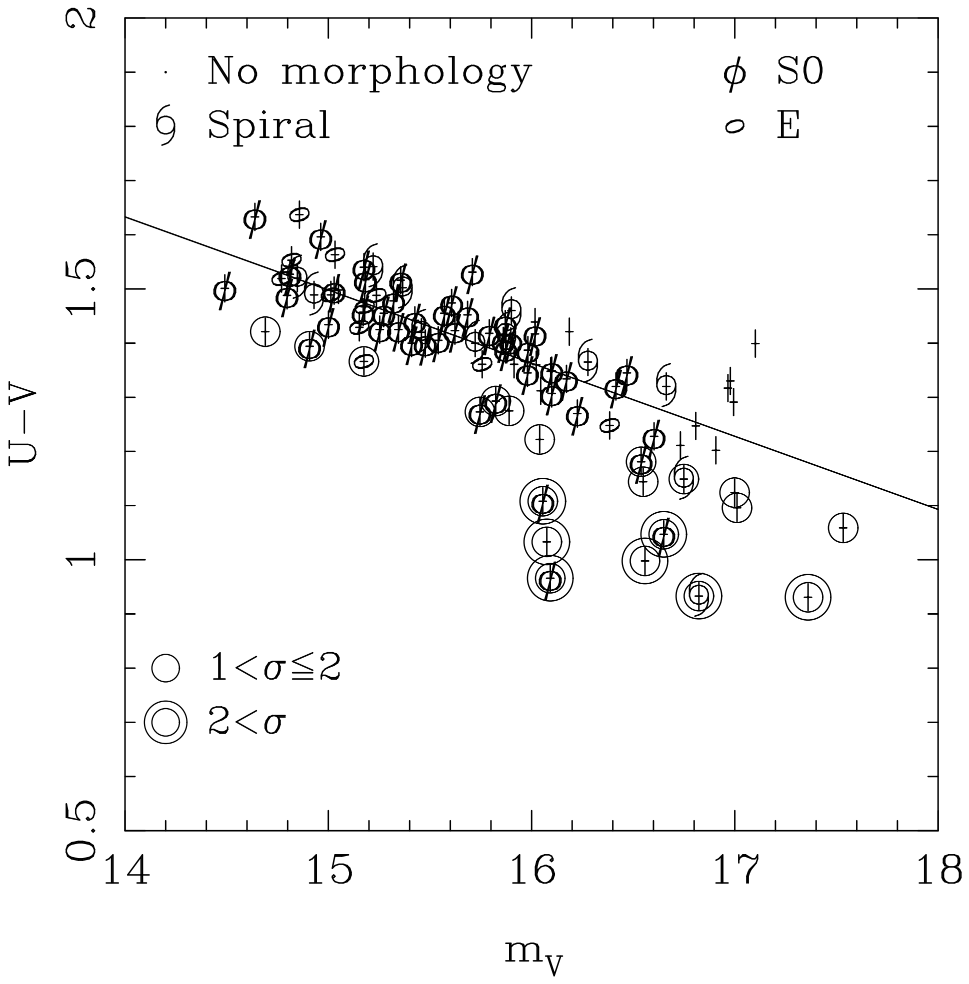

Fig. 1.2. The $U-V$ CMR relation for 101 Coma galaxies. Colors and magnitudes are within an 8!8-diameter aperture. The standard deviation about the best fit (solid line) is 0.07±0.01 mag. The symbols are coded by the morphological type of each galaxy. Galaxies that lie between 1 and 2 standard deviations blueward of the CMR best fit have an additional circle drawn around the symbol. Galaxies that lie more than 2 standard deviations blueward of the CMR best fit have two extra circles. (Taken from Terlevich et al. 1999.)

the Coma $U-V$ vs. V relation by almost two magnitudes and discovered a substantially increased scatter among the fainter population (see Fig. 1.2). Furthermore, they used metal- and Balmer-line index measurements, together with broad-band colors, to interpret the CMR in terms of changes in age and metalicity, using the stellar population models of Worthey (1994) and Worthey & Ottaviani (1997). They showed that the change in color over the most luminous decade of the CMR can be accounted for by roughly a factor of 2 increase in metalicity; a similar result was found by Vazdekis et al. (2001) for the Virgo cluster. To account for the blueward scatter of the fainter galaxy population, however, they needed to

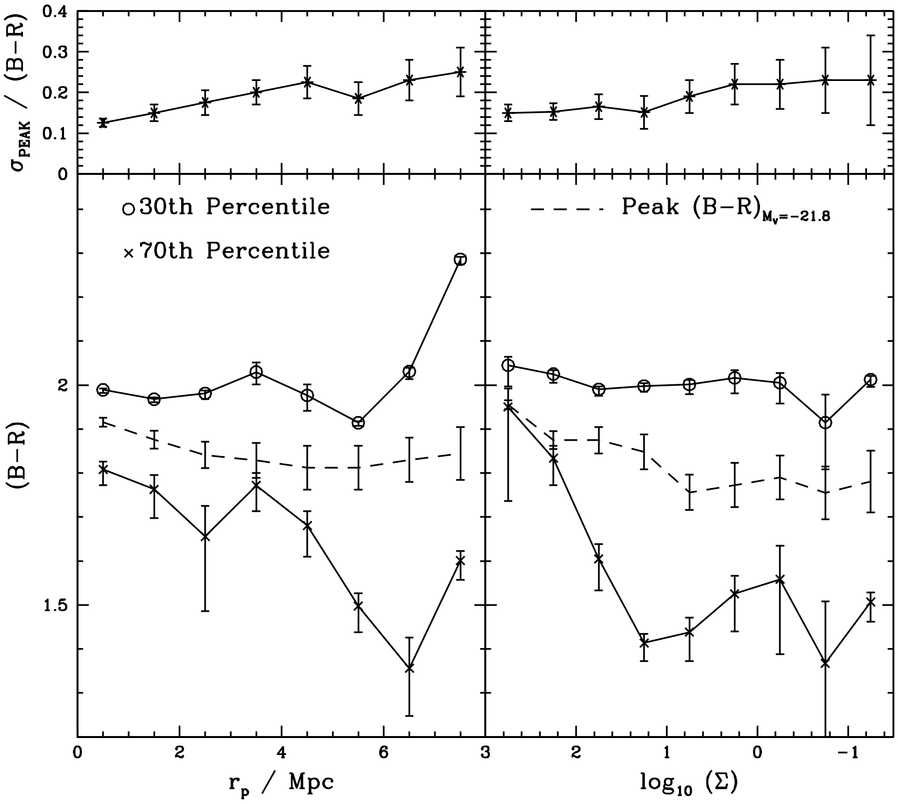

Fig. 1.3. $B-R$ color as a function of cluster radius and local density (lower panels). The three lines represent the peak, 30th, and 70th percentiles of the color histograms measured relative to the red end of the distribution. The 30th percentile of the distributions is nearly constant over at least the inner 6 Mpc of the combined cluster, while the peak shifts to the blue. The upper panel displays the width of the Gaussian fit to the color histograms against radius and local galaxy density. (Taken from Pimbblet et al. 2002).

add a population of young stars. They demonstrated that the stronger Balmer lines and bluer colors could be accounted for by a population of 1 Gyr old stars containing 15% of the mass.

Terlevich, Caldwell, & Bower (2001) explored variations in the CMR as a function of radius in the Coma cluster and found that the slope remains constant as a function of radius, but that at fixed luminosity the colors get bluer toward the outskirts. This is a small but significant effect, which they were not able to account for simply on the basis of dust in the cluster, as this would produce too much scatter in the CMR compared to the data. They concluded that the galaxies up to 1 Mpc from the cluster center have younger luminosity-weighted ages by at most 2 Gyr compared to those in the core. Pimbblet et al. (2002), reporting the results of the LARCS project, extended the study of the CMR as a function of radius to a homogeneous sample of 11 luminous X-ray clusters at $z \approx 0.1$. By combining the galaxy populations of the clusters, they were able to extend the investigation to much larger radii, out to 6 Mpc. They found that, although the position of the red envelope of the CMR does not vary as a function of projected radius (or local galaxy density), the modal colors of galaxies lying on the CMR become bluer with increasing projected radius or decreasing density (see Fig. 1.3). They inferred that as projected radius increases the red envelope remains unchanged but the fraction of bluer galaxies increases. They concluded that toward the periphery of clusters there is an increasing fraction of galaxies that exhibit signatures of star formation in the recent past and that this characteristic is not present in the evolved galaxies in the highest density regions of the clusters.

1.3.2 The Star Formation Rate in Local Clusters

The local CMR results have been extended to measurements of the star formation rate through the work of the 2dF and SDSS redshift survey teams (Lewis et al. 2002; Gomez et al. 2003). Lewis et al. (2002) made Hα emission-line equivalent width measurements for 11,006 galaxies brighter than $M_B = -19$ mag in 17 known rich clusters with $0.05 < z < 0.1$. They deduced the star formation rate, normalized to L^*, as a function of distance from the cluster center and found that it is skewed toward larger values with increasing radius, reaching the value for the field population at distances greater than three times the virial radius. They found a correlation between normalized star formation rate and local projected density (Fig. 1.4), which saturates at projected densities below about 1 galaxy Mpc^{-2}, for galaxies brighter than $M_B = -19$, corresponding roughly to the mean density at the cluster virial radius. Importantly, they were able to establish that this relation between star formation rate and local density is valid in density enhancements that are more than two virial radii from the cluster center. Therefore, they concluded that environmental influences on galaxy properties are not restricted to cluster cores, but are effective in all groups where the density exceeds a critical value.

1.3.3 The Color-Magnitude Relation in Clusters to $z = 1$

The remarkable uniformity of the CMR in local early-type galaxies has made it an attractive diagnostic with which to directly probe the evolution of galaxies in clusters. The availability of *HST* imaging has enabled several groups to address this. The MORPHS collaboration (Ellis et al. 1997) explored the CMR in three $z \approx 0.5$ clusters. They used *HST* images to measure the rest-frame UV–optical colors of galaxies selected on the basis of their morphology. They found a small scatter in color (<0.1 mag rms) for galaxies classified as E and E/S0, both within each cluster and from cluster to cluster. The found no trend for the scatter to increase with decreasing luminosity or any evidence for a distinction between the scatter observed for galaxies classified as ellipticals and S0. This uniformity drove them to conclude that most of the star formation in the elliptical galaxies in dense clusters was completed before $z = 3$.

Kodama et al. (1998) compiled data from *HST* on the CMR for early-type galaxies in 17 distant clusters in the redshift range 0.31–1.27 to attempt to distinguish between models in which the CMR is a sequence of increasing metalicity or age. They used the Kodama & Arimoto (1997) evolutionary model in which elliptical galaxies formed rapidly in a mono-

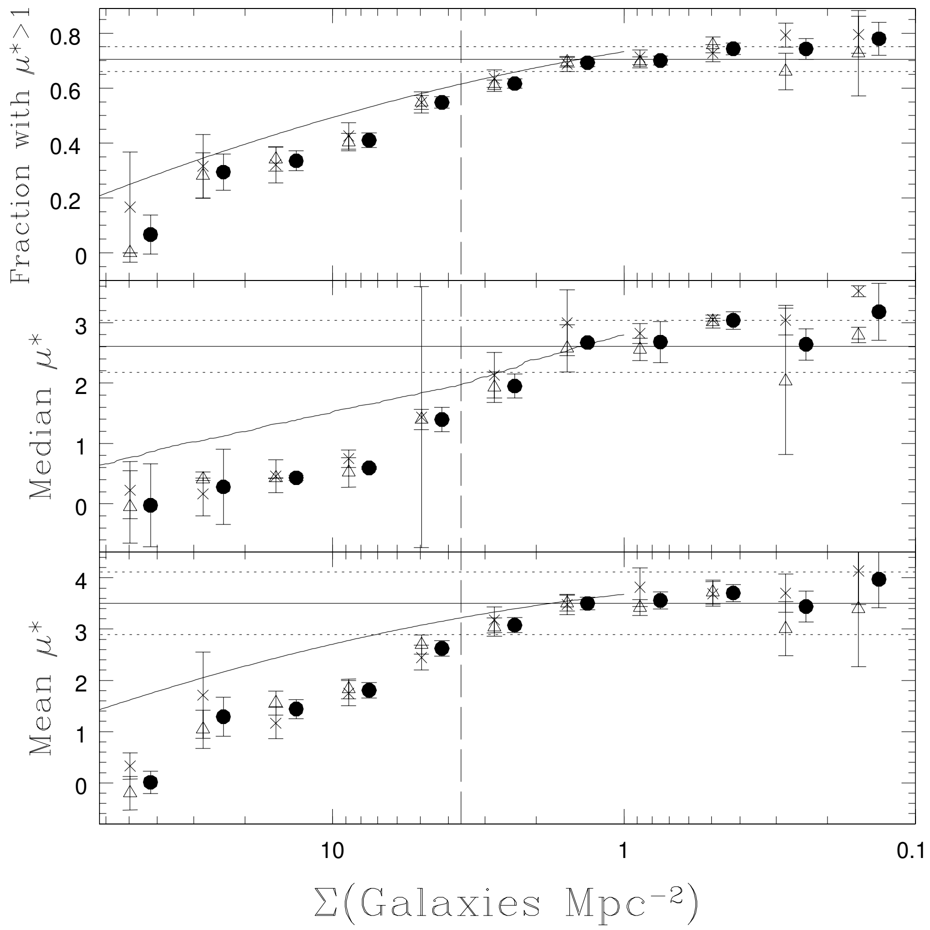

Fig. 1.4. Normalized star formation rate, μ^* as a function of local projected density. The bottom and middle panels show the mean and median value of μ^* in the cluster sample. The top panel shows the fraction of galaxies with $\mu^* > 1 M_\odot\,\mathrm{yr}^{-1}$. Solid points represent the full galaxy sample, while the triangles and crosses are from clusters with velocity dispersion greater or less than 800 km s^{-1}, respectively (offset in density for clarity). The horizontal, solid line represents the value of each statistic in the field sample; the dotted lines are an estimate of the field-to-field standard deviation. The vertical, dashed line represents the mean projected density of galaxies within the virial radius of the cluster. The solid curves are the expected trends due to the morphology-density relation of Dressler (1980), assuming the field population is composed of 18% E, 23% S0, and 59% spiral galaxies (Whitmore, Gilmore, & Jones 1993). (Taken from Lewis et al. 2002.)

lithic collapse followed by a galactic wind. They were able to reproduce the CMR for Coma ellipticals by assuming they formed either a metalicity sequence or an age sequence. They then used the model to predict the slope and zeropoint of the CMR as a function of redshift under the two hypotheses. By assuming all elliptical galaxies are coeval with a mean stellar metalicity that increases with luminosity, they found no significant differences between the CMR of the clusters and the models. They used the zeropoint of the CMRs to constrain the epoch of major star formation in early-type galaxies to $z \approx 4$.

In a complementary study, Gladders et al. (1998), measured the slope of the red sequence of galaxies in 44 Abell clusters at $z < 0.15$ and used these as a control sample for comparison with six clusters with *HST* imaging in the range $0.2 < z < 0.75$. The Kodama & Arimoto (1997) models predict a change in the observed slope of the red sequence of elliptical galaxies as a function of redshift because as galaxies age the metal-rich systems become redder faster than the more metal-poor ones. Specifically, we expect the red sequence to be significantly flatter up to 4 Gyr after formation than at later times. Thus Gladders et al. used the *slope* of the red sequence to constrain the formation epoch of cluster galaxies and did not need to rely on precise absolute photometry to determine the zeropoints. They detected the expected steepening with increasing redshift and concluded that the galaxies could not have formed more recently than $z = 2$.

Both the local CMR studies and those of clusters to $z = 1$ conclude that the luminous early-type galaxies in cluster cores formed at early epochs and that secondary star formation is rare. There is strong evidence that an increase in metalicity with luminosity is responsible for the CMR. However, it is also clear that for lower luminosity galaxies and galaxies away from the cluster core secondary star formation is more common and results in a larger fraction of blue galaxies and more scatter in the CMR. The results of emission-line determinations of star formation rate confirm these results and have shown that there is a threshold density above which star formation is quenched. This density is remarkably low, suggesting that physical mechanisms that work *only* in the dense regions of cluster cores, such as ram presure stripping, cannot be entirely responsible for the observed changes.

1.3.4 The Fundamental Plane

The fundamental plane (FP) links the velocity dispersion of the stars to the size and surface brightness of elliptical galaxies. It was discovered through studying the early-type galaxy population of clusters in the late 1980s (Djorgovski & Davis 1987; Dressler et al. 1987), and it has been used as a distance indicator to measure cluster peculiar motions (e.g., Faber et al. 1989; Colless et al. 1999; Hudson et al. 2001). Colless et al. (2001) report the following relationship based on their 29 best-observed clusters:

$$\log\, R_e = 1.22 \log\, \sigma + 0.33\langle\mu_e\rangle - 8.66,$$

where R_e is the effective radius, $\langle\mu_e\rangle$ is the mean R-band surface brightness inside R_e, and σ is the central velocity dispersion. The zeropoint is essentially that which gives the Coma cluster zero peculiar velocity. Elliptical galaxies fall on this plane with very little scatter, 0.064 in $\log\, R_e$. The FP can be used as an indicator of the homogeneity of the stellar population of cluster galaxies. Its small scatter was used by Ciotti & Renzini (1993) to estimate that the range in mass-to-light ratio (M/L) at any given location in the plane is only 12%. In their analysis of the κ-space distribution, Bender, Burstein, & Faber (1992) estimated an increase in blue M/L, from 5 to 10, over the absolute magnitude range from –20.5 to –23.5. They argued that the scatter in age and/or metalicity at fixed σ must be less than 15%. Colless et al. (1999) similarly demonstrated that the small scatter in the FP constrains the range of ages of early-type galaxies in clusters to $\pm 30\%$ (as long as there is no strong anticorrelation between age and metalicity). These remarkably uniform properties stimulated work to measure the evolution of galaxies directly by measuring the FP for clusters at redshifts up to $z \approx 1$. Such work relies on *HST* imaging to make measurements of R_e and large ground-based telescopes to measure the stellar velocity dispersions. Jørgensen et al. (1999) compared the FP for six clusters out to $z = 0.58$. They find that the scatter around the FP is similar for all six clusters and that the mass-to-light ratio decreases with redshift: log $(M/L)_r = -0.26 \pm 0.06\Delta z$, consistent with passive evolution of a stellar population that formed at a redshift larger than 5.

Franx et al. (2000) and van Dokkum et al. (2000) extended this work to $z = 0.83$, finding that early-type galaxies in clusters follow a well-defined relation out to the highest redshift and confirming that the mass-to-light ratio evolution is slow. They considered this result in the context of current galaxy evolution models involving mergers, starbursts, and the resulting changes in morphology and luminosity. They speculated that the youngest early-type galaxies at low redshift have different (pre-merger) morphological types at high redshift and therefore do not appear in high-redshift samples of early-type galaxies; they dubbed this a ''progenitor bias.'' They noted that there is a high fraction of close companions or merging galaxies in the periphery of their highest redshift clusters, a number comparable to the fraction of ellipticals. These merger candidates fall on the same CMR as the ellipticals but have roughly twice the scatter. These results suggest that the present-day population of early-type galaxies in clusters has not been constant, but is evolving, and that ellipticals are created as galaxy pairs or groups fall into clusters. This picture is qualitatively consistent with the low-redshift result that the star formation rate increases monotonically with radius in clusters and suggests that roughly half the population of cluster ellipticals has assembled since $z = 1$. In a follow-up study, Kelson et al. (2001) measured the velocity dispersions and Balmer absorption-line strengths of galaxies in four clusters with $0.06 < z < 0.83$ and found that the evolution of the Balmer-line strength at fixed σ was consistent with passive evolution of single stellar population models and similar to that derived from the FP, once again requiring an early redshift of formation.

1.3.5 Line Strengths: The Age/Metalicity Dilemma

Models of the integrated spectral energy distributions of old stellar populations exhibit a degeneracy between increasing the age and increasing the metalicity of the population, such that it has been difficult to distinguish between changes in these on the basis of, for example, broad-band colors alone. This problem provided the motivation for studies of the CMR and FP to make measurements at high redshift where these two factors can be separated. In the 1990s models became available that identified index combinations, such as Hβ and an average of iron and magnesium features ([MgFe]), which together have some leverage between age and metalicity (Worthey 1994). This enabled age and metalicity to be determined in local galaxies using high-precision spectroscopy. These models were expanded and refined throughout the last decade (Worthey & Ottaviani 1997; Vazdekis 1999) so that we now have a powerful set of tools to address questions of the age and metalicity of local galaxies. Some of these models have even been developed to include relative abundances that are not in the solar ratios, to address some anomalies in the standard model fits (e.g., Thomas, Maraston, & Bender 2003).

The first application of the Worthey models was by González (1993) who analyzed long-slit spectra of 41 elliptical galaxies taken with a CCD system at Lick Observatory. The

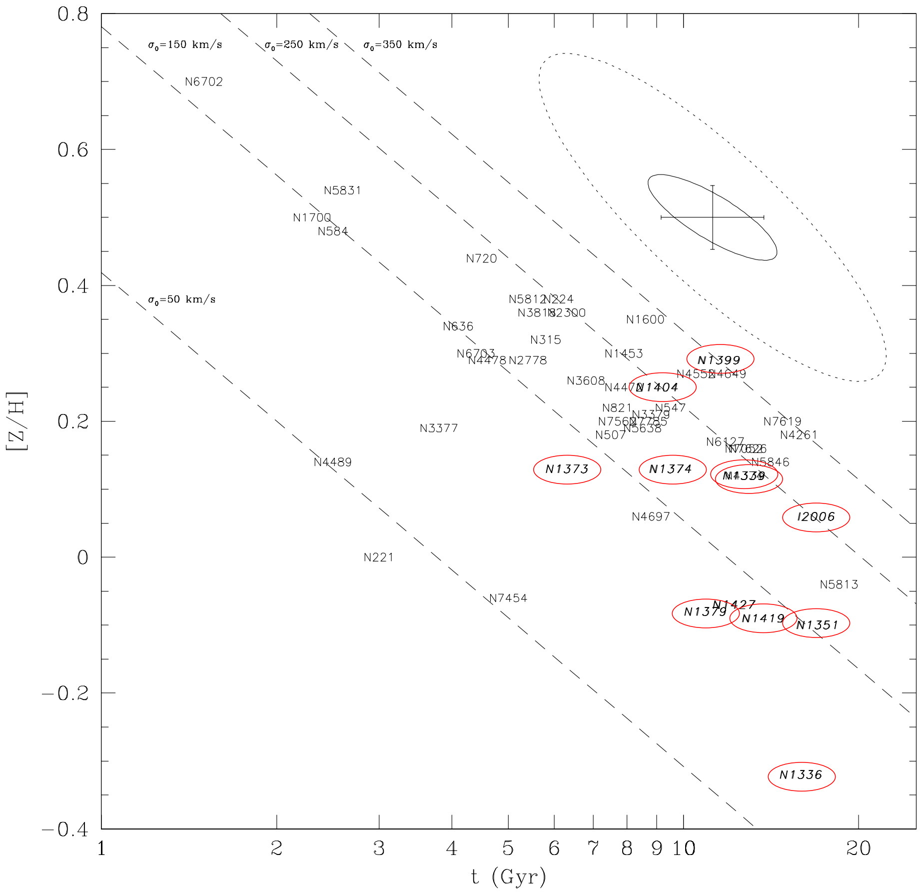

Fig. 1.5. A face-on view of the “Z-plane” from Trager et al. (2000), adapted to highlight the Fornax elliptical galaxies from Kuntschner & Davies (1998). At fixed velocity dispersion (dashed lines), younger galaxies have higher metalicities than older galaxies. The solid error ellipse in the top right-hand corner is typical of the González (1993) sample; the dotted ellipse is typical of the highest quality data in the Lick/IDS galaxy sample (Trager et al. 1998). The slope of the error ellipses is nearly identical to the of lines of constant velocity dispersion, indicating that poor data can masquerade as a real trend. The Fornax ellipticals are ringed and can be seen to be coeval within the uncertainty of the best data.

sample of galaxies in González’s thesis exhibited a factor of 10 range in age, while spanning only a factor of 2–3 in metalicity. These galaxies were much closer to an age sequence than a metalicity sequence, in contradiction to the view developed from cluster CMR and FP studies, although the sample was drawn from the full range of environments in which ellipticals are found. In contrast, Kuntschner & Davies (1998) found that in the Fornax cluster the elliptical galaxies fall on a tight metalicity sequence of constant age, whereas the lenticular galaxies scatter to luminosity-weighted ages as young as 2 Gyr. González’s

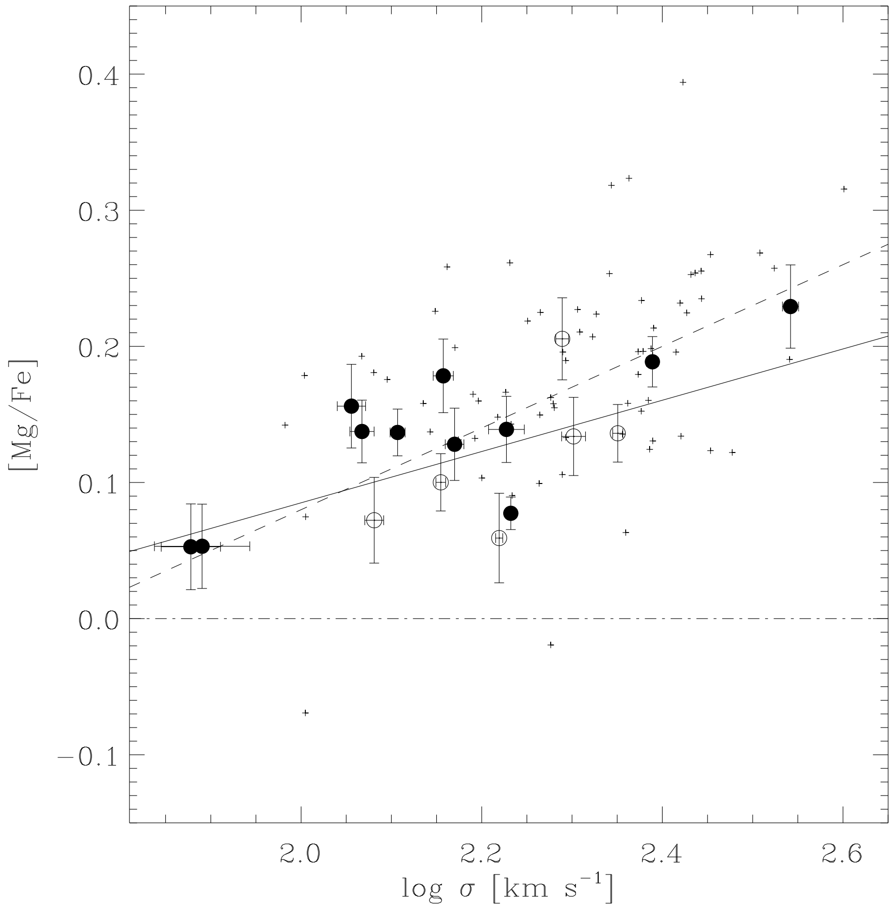

Fig. 1.6. The relationship between [Mg/Fe] and log σ for galaxies in the Fornax cluster (large symbols: filled circles are elliptical galaxies, open circles are S0 galaxies); the best fit to these data is the solid line. The sample compiled by Kuntschner et al. (2001), which is dominated by galaxies in the Coma and Virgo clusters, is shown as crosses; the best fit to these data is the dashed line. This figure is adapted from Figure 16 of Kuntschner et al. (2002).

work was re-visited by Trager et al. (2000), who included galaxies from the Kuntschner & Davies sample. As illustrated in Figure 1.5, they found that at fixed σ there is an anticorrelation between age and metalicity. They demonstrated that this anticorrelation can account for the tightness of the Mg-σ relation because if galaxies experience secondary star formation (changing their mean age) they move along the relation rather increasing the scatter. I have therefore not included this relationship among those used to argue that luminous cluster ellipticals are old. Trager et al., however, agreed that the ellipticals in clusters are predominantly old and that it is the low-luminosity galaxies and galaxies in lower density regions

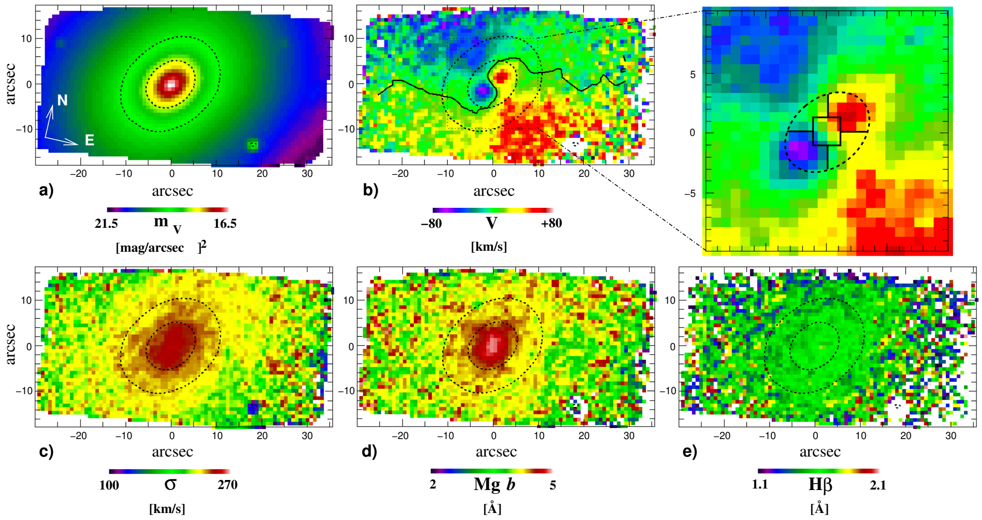

Fig. 1.7. Maps of (a) reconstructed surface brightness; (b) mean streaming velocity V, (c) velocity dispersion σ, (d) Mg b line strength, and (e) Hβ line strength for NGC 4365. Isophotal contours of μ_V = 18 and 19 mag arcsec^{-2} are overplotted (dotted lines). A zero-velocity contour line (solid black line) is shown in (b). The enlarged core region of the velocity map indicates the regions used for line-strength analysis; see Figure 1.8. The central point is indicated by the square, the decoupled core by the sectors along the major axis, and the main body at the same radius by the sectors along the minor axis. (Taken from Davies et al. 2001.)

that have experienced secondary star formation, which they referred to as a "frosting" of younger stars. Recently, Kuntschner et al. (2002) have carried out a similar analysis on a sample of ellipticals drawn from extreme low-density environments and shown that indeed they have younger luminosity-weighted ages than cluster galaxies.

One failing of the single stellar population models is that they are not able to account for the strength of the magnesium absorption features in metal-rich populations. This is why most of the above analysis is done using a combination of magnesium and iron lines. Over the last 15 years we have come to realize that the abundance patterns in early-type populations is not solar and that the magnesium-to-iron ratio is enhanced compared to solar values (Peletier 1989; Worthey, Faber, & Gonzáles 1992; Davies, Sadler, & Peletier 1993). A number of possible origins for this abundance pattern were considered, and the consensus view is that the overabundance arises from magnesium production in Type II supernovae that occurred in a burst of star formation lasting less than 1–2 Gyr, perhaps considerably less. The iron, which is produced primarily in Type Ia supernovae at later times, does not enrich the population because by then star formation has ceased, for example by the onset of a galactic wind. Trager et al. used models that include a parameterization of the overabundance [E/Fe], based on corrections to the Worthey models (Tripicco & Bell 1995), to estimate the level of enhanced abundances and concluded that elliptical galaxies fall on a plane in the four-space of velocity dispersion (log σ), age (log t), metalicity ([Z/H]), and "enhancement" ratio ([E/Fe]). They decomposed this plane into the "Z-plane" (Fig. 1.5) and the [E/Fe]

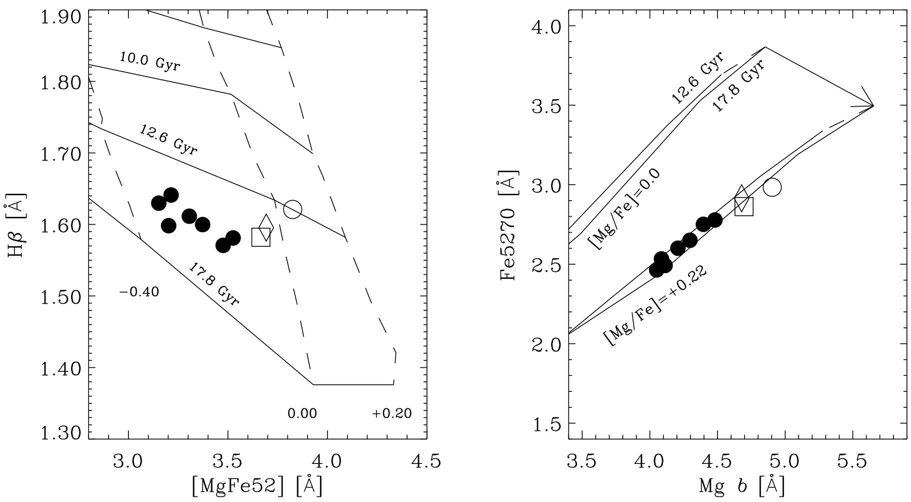

Fig. 1.8. *Left:* [MgFe52] vs. Hβ equivalent width diagram. The open circle represents the average line strength of the very central data points ($r < 1\farcs6$), the open diamond represents the region of the decoupled core, and the open square is the mean of the data in the main body of the galaxy at the same radii as the decoupled core but along the minor axis (see also Fig. 1.7, enlarged core region). For larger radii, the data were averaged in elliptical annuli centered on the photometric nucleus (filled circles) from $5\farcs6$ to $26\farcs1$. Overplotted are the predictions of stellar population models from Vazdekis (1999). The solid lines are lines of constant age, and the dashed lines are lines of constant metalicity. *Right:* Mg *b* vs. Fe5270 equivalent width diagram. Overplotted are stellar population models from Vazdekis (1999) with solar abundance ratios for ages of 12.6 and 17.8 Gyr, which are degenerate. In addition, a correction of the models for nonsolar abundance ratios, of [Mg/Fe] = 0.22 dex, is shown (Trager et al. 2000). The error bars on the mean line strength in a given zone are omitted for clarity, as they are similar to the size of the symbols in the diagrams. (Adapted from Davies et al. 2001.)

vs. log σ plane. Figure 1.6, adapted from Kuntschner et al. (2002), shows [Mg/Fe] as a function of log σ for the Fornax galaxies and those compiled in Kuntschner et al. (2001), a sample dominated by galaxies in the Coma and Virgo clusters. This relationship shows that the high-velocity dispersion galaxies in clusters have a systematic overabundance of magnesium, which implies a short time scale for star formation in these systems (Bender 1996).

1.4 The Decoupled Core in NGC 4365

To address the issue of how and when galaxies assembled, we would ideally need to estimate the age of each stellar component of a galaxy to determine, for example, whether the core formed earlier or later than the bulk of the galaxy, or whether disks form stars over a longer period than bulges. To understand how galaxies assemble, we need to order the formation events. The results I have discussed so far arise from measurements of central or integrated values of color, dispersion, line strength, etc., and so are not able to address the formation epoch of different stellar components. Integral-field spectrographs, however, provide maps of these quantities at each point across the face of a galaxy. The SAURON spectrograph (Bacon et al. 2001) was built to carry out these studies and has been used in an extensive survey designed to characterize the local early-type galaxy population in terms of luminosity, environment, and morphology (de Zeeuw et al. 2002). The potential of such measurements is well illustrated by their maps of NGC 4365, an elliptical galaxy with a decoupled core (Davies et al. 2001). In Figure 1.7, we see that the velocity maps show two independent kinematic subsystems: the central 300 pc $\times$ 700 pc rotates about the projected minor axis, and the main body of the galaxy (3 kpc $\times$ 4 kpc) rotates almost at right angles to this. The misalignment between the photometric and kinematic axes of the main body is unambiguous evidence of triaxiality. Remarkably, the decoupled core does not show a signature in the line-strength maps. Figure 1.8*a* shows that the metalicity of the stellar population decreases from a central value greater than solar to one-half solar at a radius of 2 kpc. The Vazdekis (1999) models imply that the decoupled core and main body of the galaxy have the same luminosity-weighted age, 14 Gyr. In Figure 1.8*b* we see that the whole galaxy possesses the same elevated magnesium-to-iron ratio. The two kinematically distinct components have thus shared a common star formation history. We infer that the galaxy underwent a sequence of mergers associated with dissipative star formation that ended roughly 12 Gyr ago. The similarity of the stellar populations in the two components suggests that the observed kinematic structure has not changed substantially in 12 Gyr.

1.5 Summary

(1) Direct measurements of intracluster stars show that they account for 10%–20% of the total stellar luminosity of clusters.

(2) There is strong evidence that the population of luminous, high-dispersion galaxies in rich clusters is old and forms a metalicity sequence (the CMR and FP, both locally and to $z \approx 1$, the Hα-inferred star formation rate, the line-strength analysis of age and metalicity). Furthermore, the increasing enhancement of magnesium abundance in high-dispersion galaxies implies short star formation time scales in these galaxies. These observations are counter to the hierarchical picture of galaxy assembly in which the most massive objects assemble latest. They suggest that massive early-type galaxies in clusters formed by an alternative route; the short time scale for formation suggests a scheme similar to the monolithic collapse modeled by Larson (1975) and Carlberg (1984). One caveat is that the very central, brightest cluster galaxies frequently show emission lines, nuclear activity, and evidence for secondary star formation, which are associated with their special location at the center of the cluster potential. With this exception, luminous cluster ellipticals appear to be the quiescent remnants of an early starburst. This early phase has recently been invoked to account for the high star formation rates implied for the SCUBA sources (e.g., Smail et al. 2003).

(3) For lower luminosity galaxies ($\sigma < 150$ km s^{-1}) and galaxies found in the outer reaches (lower density environments) of clusters, the same evidence shows that secondary star formation has played an important role in their evolution. It seems likely that these galaxies have assembled hierarchically. The low star formation rates found at large cluster radius (low density) rule out physical processes that require high gas densities to operate, such as ram pressure stripping of disk gas, as being completely responsible for the variations in galaxy properties with environment.

(4) The availability of integral-field spectrographs that can map the kinematics and stellar popu-

Fig. 1.9. The "Ashby Free Library" in Ashby, North Lincolnshire. This photograph was taken shortly after it opened in 1904. The library was built using a £1500 donation from Andrew Carnegie. The author spent many childhood hours in this library, including those spent on his first astronomy project. Thanks to Carol Longbone of North Lincolnshire Libraries for providing the photograph.

lations of galaxy components offers the potential for directly measuring the assembly history of galaxies.

Acknowledgements. I would like to thank the PPARC for the award of a Senior Fellowship and the University of Oxford for research support. I am pleased to thank Harald Kuntschner and Marc Sarzi for assistance with the production of Figures 1.6 and 1.8. I am grateful to Carol Longbone and North Lincolnshire Libraries and Information Services who provided Figure 1.9.

References

Arnaboldi, M., et al. 2003 AJ, 125, 514
Bacon, R., et al. 2001 MNRAS, 326, 23
Bender, R. 1996, in IAU Symp. 171, New Light on Galaxy Evolution, ed. R. L. Davies & R. Bender (Dordrecht: Kluwer), 181
Bender, R., Burstein, D., & Faber, S. M. 1992, ApJ, 399, 462
Binggeli, B., Sandage, A. R., & Tammann, G. A. 1987, AJ, 94, 251
Bower, R. G., Lucey, J. R., & Ellis, R. S. 1992, MNRAS, 254, 589
Bruzual A., G. 1983, ApJ, 273, 105
Carlberg, R. G. 1984, ApJ, 286, 403
Ciotti, L., & Renzini, A. 1993, ApJ, 416, L49
Colless, M., Burstein, D., Davies, R. L., McMahan, R. K., Jr., Saglia, R. P., & Wegner, G. 1999, MNRAS, 303, 813
Colless, M., Saglia, R. P., Burstein, D., Davies, R. L., McMahan, R. K., Jr., & Wegner, G. 2001 MNRAS, 321, 277
Conselice, C. J., Gallagher, J. S., III, & Wyse, R. F. G. 2003, AJ, 125, 66
Davies, R. L., et al. 2001, ApJ, 548, L33
Davies, R. L., Sadler, E. M., & Peletier, R. F. 1993, MNRAS, 262, 650
de Zeeuw, P. T., et al. 2002 MNRAS, 329, 513
Djorgovski, S. G., & Davis, M. 1987, ApJ, 313, 59
Dressler, A. 1980, ApJ, 236, 351
Dressler, A., Gunn, J. E., & Schneider, D. P. 1985, ApJ, 294, 70
Dressler, A., Lynden-Bell, D., Burstein, D., Davies, R. L., Faber, S. M., Terlevich, R., & Wegner, G. 1987, ApJ, 313, 42
Durrell, P. R., Ciardullo, R., Feldmeier, J. J., Jacoby, G. H., & Sigurdsson, S. 2002, ApJ, 570, 119
Ellis, R. S., Smail, I., Dressler, A., Couch, W. J., Oemler, A., Jr., Butcher, H., & Sharples, R. M. 1997, ApJ, 483, 582
Faber, S. M., Wegner, G., Burstein, D., Davies, R. L., Dressler, A., Lynden-Bell, D., & Terlevich, R. J. 1989, ApJS, 69, 763
Feldmeier, J. J., Mihos, J. C., Morrison, H. L., Harding, P., & Kaib, N. 2004, in Carnegie Observatories Astrophysics Series, Vol. 3: Clusters of Galaxies: Probes of Cosmological Structure and Galaxy Evolution, ed. J. S. Mulchaey, A. Dressler, & A. Oemler (Pasadena: Carnegie Observatories, http://www.ociw.edu/ociw/symposia/series/symposium3/proceedings.html)
Feldmeier, J. J., Mihos, J. C., Morrison, H. L., Rodney, S. A., & Harding, P. 2002, ApJ, 575, 779
Ferguson, A. M. N., Tanvir, N. R., & von Hippel, T. 1998, Nature, 391, 461
Franx, M., van Dokkum, P. G., Kelson, D., Fabricant D. G., & Illingworth, G. D. 2000, Philosophical Transactions: Mathematical, Physical & Engineering Sciences, 358, 2109
Gladders, M. D., Lopez-Cruz, O., Yee, H. K. C., & Kodama, T. 1998, ApJ, 501, 571
Gomez, P. L., et al. 2003, ApJ, 584, 210
González, J. J. 1993, Ph.D. Thesis, University of California, Santa Cruz
Harris, W. E., Kavelaars, J. J., Hanes, D. A., Hesser, J. E., & Pritchet, C. J. 2000, ApJ, 533, 137
Hudson, M. J., Lucey, J. R., Smith, R. J., Schlegel, D. J., & Davies, R. L. 2001, MNRAS, 327, 265
Jørgensen, I., Franx, M., Hjorth, J., & van Dokkum, P. G. 1999, MNRAS, 308, 833
Kelson, D. D., Illingworth, G. D., Franx, M., & van Dokkum, P. G. 2001, ApJ, 552, L17
Kodama, T., & Arimoto, N. 1997, A&A, 320, 41
Kodama, T., Arimoto, N., Barger, A. J., & Aragón-Salamanca, A. 1998, A&A, 334, 99
Kuntschner, H., & Davies, R. L. 1998, MNRAS, 295, L29
Kuntschner, H., Lucey, J. R., Smith, R. J., Hudson, M. J., & Davies, R. L. 2001, MNRAS, 323, 615
Kuntschner, H., Smith, R. J., Colless, M., Davies, R. L., Kaldare, R., & Vazdekis, A. 2002, MNRAS, 337, 172
Larson, R. B. 1975, MNRAS, 173, 671
Lewis, I. J., et al. 2002, MNRAS, 334, 673

Moore, B., Katz, N., Lake, G., Dressler, A., & Oemler, A. 1996, Nature, 379, 613
Peletier, R. F. 1989, Ph.D. Thesis, University of Groningen
Pimbblet, K. A., Smail, I., Kodama, T., Couch, W. J., Edge, A. C., Zabludoff, A. I., & O'Hely, E. 2002, MNRAS, 331, 333
Sandage, A. 1972, ApJ, 176, 21
Schneider, D. P., Gunn, J. E., & Hoessel, J. G. 1983, ApJ, 264, 337
Shectman, S. 1973, ApJ, 179, 681
——. 1974, ApJ, 188, 233
Smail, I., Ivison, R. J., Gilbank, D. G., Dunlop, J. S., Keel, W. C., Motohara, K., & Stevens, J. A. 2003, ApJ, 583, 551
Terlevich, A. I., Caldwell, N., & Bower, R. G. 2001, MNRAS, 326, 1547
Terlevich, A. I., Kuntschner, H., Bower, R. G., Caldwell, N., & Sharples, R. M. 1999, MNRAS, 310, 445
Theuns, T., & Warren, S. J. 1997, MNRAS, 284, L11
Thomas, D., Maraston, C., & Bender, R. 2003, MNRAS, 339, 897
Trager, S. C., Faber, S. M., Worthey, G., & González, J. J. 2000, AJ, 120, 165
Trager, S. C., Worthey, G., Faber, S. M., Burstein, D., & González, J. J. 1998, ApJS, 116, 1
Tripicco, M. J., & Bell, R. A. 1995, AJ, 110, 3035
Uson, J. M., Boughn, S. P., & Kuhn, J. R. 1991, ApJ, 369, 46
Visvanathan, N., & Sandage, A. 1977, ApJ, 216, 214
Whitmore, B. C., Gilmore, D. M., & Jones, C. 1993, ApJ, 407, 489
Worthey, G. 1994, ApJS, 95, 107
Worthey, G., Faber, S. M., & González, J. J. 1992, ApJ, 398, 69
Worthey, G., & Ottaviani, D. L. 1997, ApJS, 111, 377
van Dokkum, P. G., Franx, M., Fabricant, D., Illingworth, G. D., & Kelson, D. D. 2000, ApJ, 541, 95
Vazdekis, A. 1999, ApJ, 513, 224
Vazdekis, A., Kuntschner, H., Davies, R. L., Arimoto, N., Nakamura, O., & Peletier, R. F. 2001, ApJ, 551, L127